Supporting information

A novel strategy to motivate the luminescent efficiency of phosphor: drilling nanoholes on the surface.

Liang-Jun Yin[1]*, Ying-Lin Liang[2]*, Sheng-Hui Zhang[1], Meng Wang[1], Langkai Li[3], Wen-Jie Xie[4], Hao Zhong[5], Xian Jian[1], Xin Xu[5], Xin Wang[6], Long-Jiang Deng[6]

[1] School of Energy Science and Engineering, University of Electronic Science and Technology of China, 2006 Xiyuan Road, Chengdu, P.R.China

[2] School of Mechatronics Engineering, University of Electronic Science and Technology of China, 2006 Xiyuan Road, Chengdu 611731, P.R.China

[3] Parkathings Amorphous Material Technology Co., Ltd, Xiamen 361005, People's Republic of China

[4] School of Materials and Chemical Engineering, Anhui Jianzhu University, Hefei, PR China

[5] Laboratory of materials for energy conversion, Department of Materials Science and Engineering, University of Science and Technology of China, Hefei, P.R.China

[6] National Engineering Research Center of Electromagnetic Radiation Control Materials, University of Electronic Science and Technology of China, 2006 Xiyuan Road, Chengdu, P.R. China
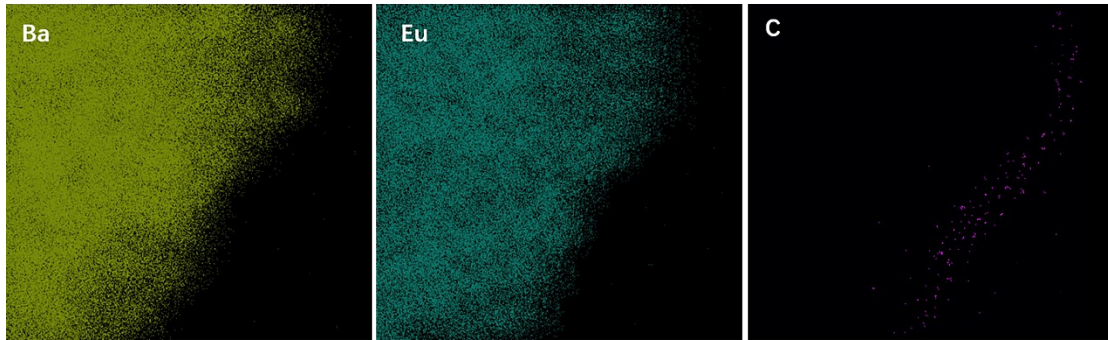
Figure S1. EDS mappings of Ba, Eu and C elements for BAM@C sample.
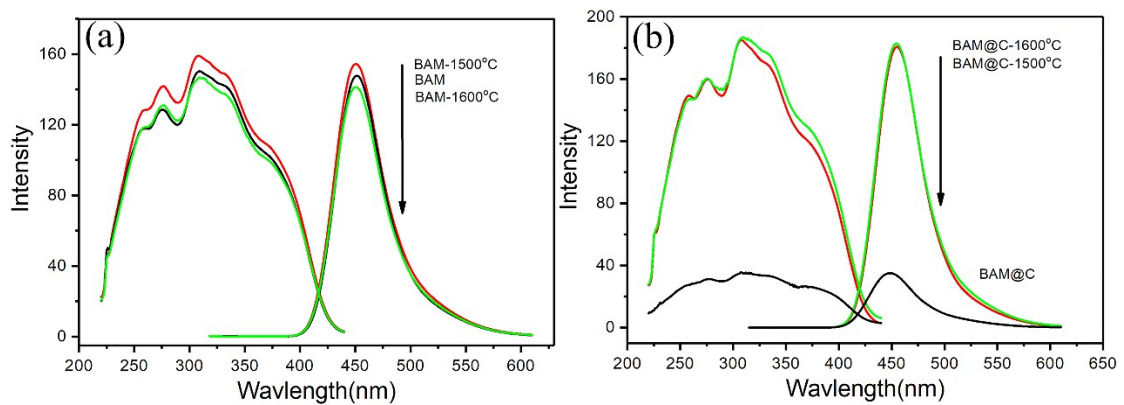
Figure S2. (a) PL measurements on post treated BAM samples ($\lambda_{ex} = 310$ nm and $\lambda_{em} = 450$ nm). (b) PL measurements on post treated BAM@C samples ($\lambda_{ex} = 310$ nm and $\lambda_{em} = 450$ nm).
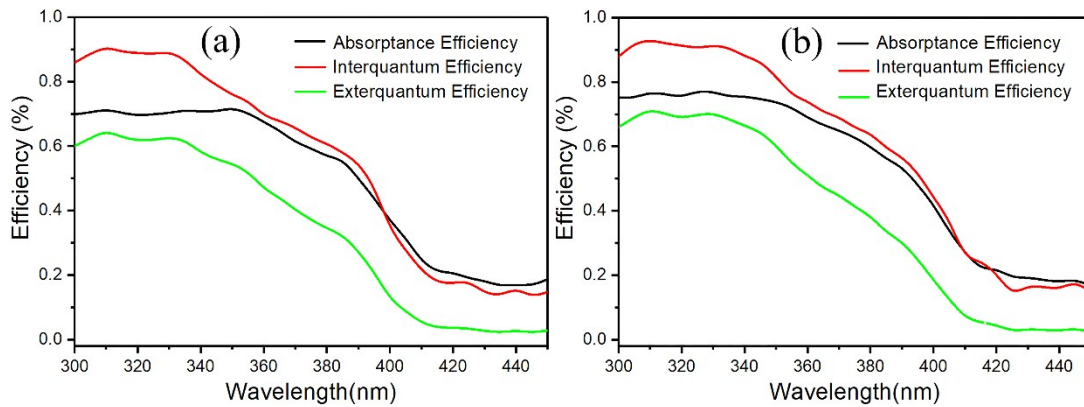
Figure S3. Quantum efficiency and absorption of BAM (a) and BAM@C-1500°C (b) samples as a function of excitation wavelength.
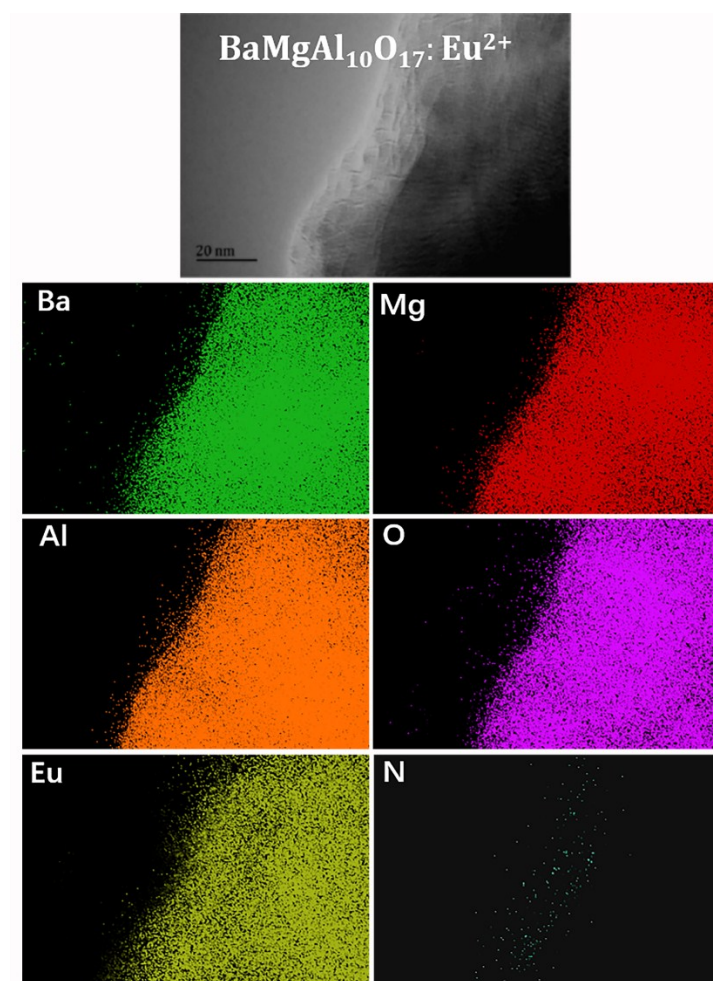
Figure S4. EDS mappings of all the elements for a BAM@C-1500ºC particle.
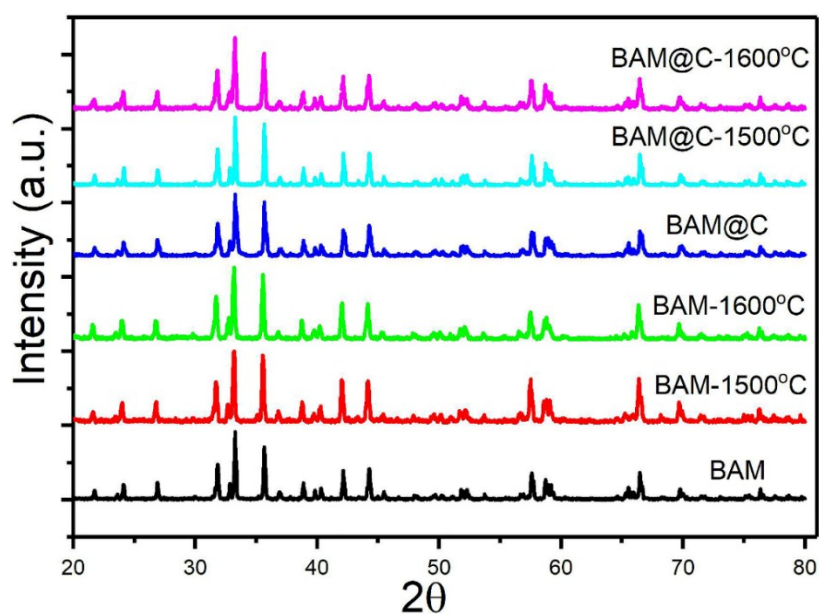
Figure S5. XRD patterns of BAM, BAM-1500ºC, BAM-1600ºC, BAM@C, BAM@C-1500ºC and BAM@C-1600ºC samples.
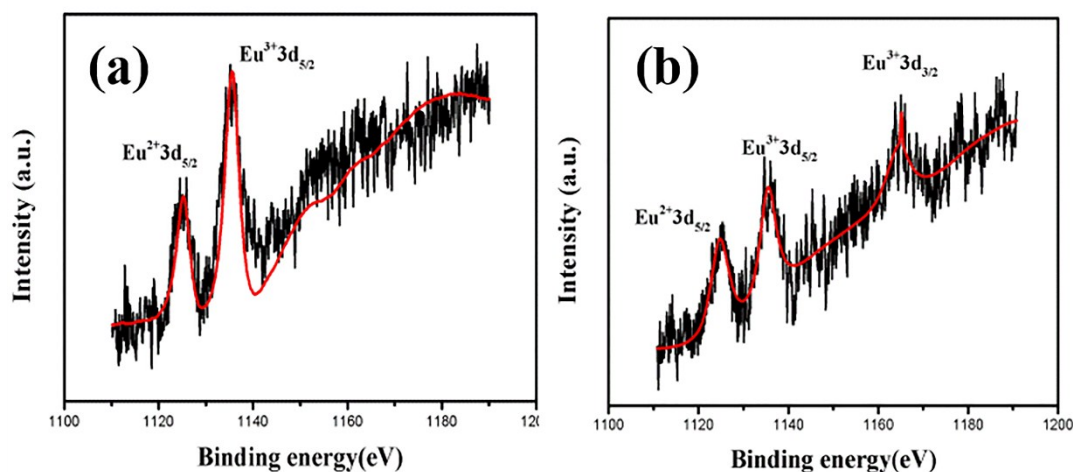
Figure S6. (a) XPS 3d spectrum of Eu in BAM@C. (b) XPS 3d spectrum of Eu in BAM@C-1500 ºC.
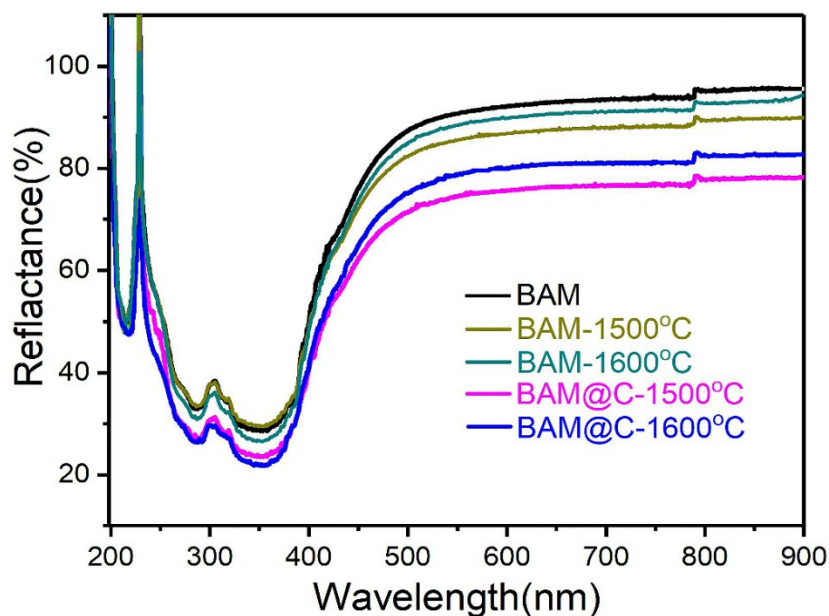
Figure S7. The reflection spectra of BAM, BAM-1500ºC, BAM@C-1600ºC, BAM@C-1500ºC and BAM@C-1600ºC.

Table 1. The mass fractions of C @ BAM and C @ BAM-1500ºC, respectively. Quantitative composition analyses were performed by combining Energy-Dispersive X-day Spectroscopy measurements (JSM-6390LA, JEOL, Japan), Nitrogen/Oxygen Analyzer (TC-436, LECO, Japan) and high frequency infrared Carbon/Sulfur analyzer (EA-CSA-05, U-THERM INTERNATIONAL, China).

Element\Sample	Eu	Ba	Mg	Al	O	N	C
BAM@C	2.16%	17.01%	3.21%	39.24%	38.19%	-	0.19%
BAM@C-1500ºC	2.28%	16.84%	3.04%	40.21%	37.58%	0.05%	0.01%

Table 2. Color Rendering Indexes and Optical Properties of wLED using treated BAM phosphor.

R1	R2	R3	R4	R5	R6	R7	R8	R9	R10	R11	R12	R13	R14	R15
93	86	89	96	91	89	94	82	52	90	94	75	86	85	76
Chromatic coordinates (x, y): (0.3425, 0.3431)														
Color temperature (K): 5077														
luminous efficacy (lm/W): 11.3														
Ra: 90														

Detained information about quantum efficiency measurement.

The quantum efficiency and absorption of the prepared samples were measured using QE-2100 photo detector with a 200 W Xe-lamp as an excitation source. The reflection spectrum of $BaSiO_4$ white standard was used for calibration. The internal (η_{in}) and external (η_{ex}) quantum efficiency of the sample were calculated based on the following equations [1]:

$$\eta_{in} = \frac{\int \lambda P(\lambda) d\lambda}{\lambda [E(\lambda) - R(\lambda)] d\lambda}$$

$$\eta_{ex} = \frac{\int \lambda P(\lambda) d\lambda}{\lambda E(\lambda) d\lambda}$$

1. K. Ohkubo and T. Shigeta, J. Illum. Eng. Inst. Jpn., 1999, 83, 87–93.

Detained information about simulations.

A 2D steady-state finite element model of frequency domain electromagnetic field is used to analyze the distribution of electric field modes in plane, which is dependent on pore diameter r and pore space dx, as shown in Figure SI 7. There is monochromatic ultraviolet light source (plane electromagnetic wave) with wavelength λ_0 =360 *nm* normal incidence on BAM material, the depth of the non-penetrating pores is 100 nm. There are some assumptions as following:

   1. The change of BAM material band structure caused by the decrease of pore size is not considered.

   2. The boundary of the simulation area is set as the scattering boundary.

   3. The incident light is a Gauss beam, and its radius is much larger than the size of BAM pore array.

   4. The optical properties of BAM are isotropic.
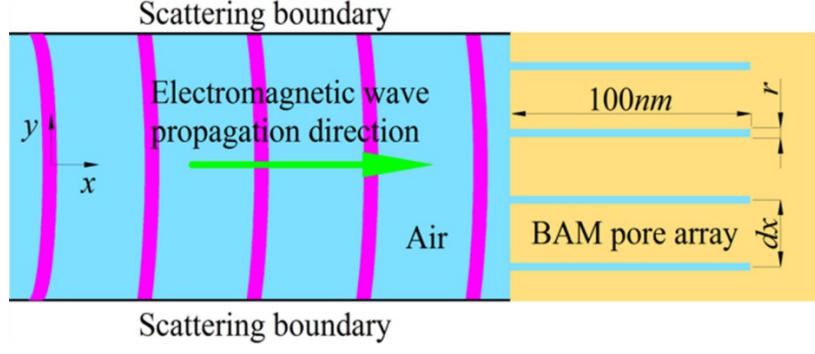
Figure SI 7. 2D steady-state finite element simulation model.

Light waves propagate in an electrically neutral and isotropic semiconductors medium, which obeys Maxwell's equations as follows

$$\begin{cases} \nabla \times E = -\mu_0 \dfrac{\partial H}{\partial t} \\ \nabla \times H = \sigma E + \varepsilon_r \varepsilon_0 \dfrac{\partial E}{\partial t} \\ \nabla \bullet H = 0 \\ \nabla \bullet D = 0 \end{cases} \tag{1}$$

Where E is electric field intensity, ε_0 and μ_0 are dielectric constant and magnetic permeability in free space respectively, ε_r is relative dielectric constant in medium, σ is electronic conductivity. So we got frequency domain governing function of the simulation model from Maxwell's equations

$$\nabla^2 E - \sigma \mu_0 \frac{\partial E}{\partial t} - \mu_0 \varepsilon_r \varepsilon_0 \frac{\partial^2 E}{\partial t^2} = 0 \tag{2}$$

In the 2D simulation model, we only consider plane electromagnetic wave propagates along the x direction, and component of the electric field in y-direction

$$E_y = E_0 e^{i\omega(t - \frac{Nx}{c_0})} \tag{3}$$

Where E_0 is wave amplitude, ω is wave angular frequency, related to light wavelength λ by $\omega = 2\pi c_0 / \lambda$, c_0 is the speed of light in vacuum. Complex refractive index $N = n - ik$, n and k are termed the refractive index and the extinction coefficient, respectively.

In calculating the governing function (2), there are two parameters depending on ω are required, $\varepsilon_r(\omega)$ and $\sigma(\omega)$, and they are related to $n(\omega)$ and $k(\omega)$ by

$\varepsilon_r(\omega) = n(\omega)^2 - k(\omega)^2$ and $\sigma(\omega) = 2\varepsilon_0 \omega n(\omega) k(\omega)$.

According to electromagnetic theory, when the light normal incidence on the demarcation surface of two different mediums, the relation between the amplitude of electricity vector of reflected light E_R, and incident light E_I and its direction can be illustrated by Fresnel formula

$$\frac{E_R}{E_I} = |r|e^{i\theta} = \frac{n - 1 - ik}{n + 1 + ik} \tag{4}$$

Since the medium absorption of light, reflection results in a phase change θ. Furthermore, separating the real and imaginary parts of equation (4), $n(\omega)$ and $k(\omega)$ which depend on ω can be calculated from the corresponding $R(\omega)$ and $\theta(\omega)$, so the following equations are obtained

$$n(\omega) = \frac{1 - R(\omega)}{1 + R(\omega) - 2\sqrt{R(\omega)}\cos\theta(\omega)} \tag{5}$$

$$k(\omega) = \frac{-2\sqrt{R(\omega)}\sin\theta(\omega)}{1 + R(\omega) - 2\sqrt{R(\omega)}\cos\theta(\omega)} \tag{6}$$

Obviously, reflectance spectrum $R(\omega)$ is easy to obtain by a spectrometer, but $\theta(\omega)$ is difficult to be measured. The principle of causality and Kramers-Kronig dispersion relation lead to a fundamental relation, what the value of $\theta(\omega)$ at any particular ω is not independent and it is directly related to the reflection spectrum by

$$\theta(\omega) = -\frac{\omega}{\pi} p \int_0^\infty \frac{\ln R(s)}{s^2 - \omega^2} ds \tag{7}$$

Which p represents Cauchy principal value integrals

$$p\int_0^\infty \equiv \lim_{\delta \to 0} \left(\int_0^{\omega - \delta} + \int_{\omega + \delta}^\infty \right) \tag{8}$$

When ω takes any value except $\omega = 0$, that

$$p\int_0^\infty \frac{1}{s^2 - \omega^2} ds = \lim_{\delta \to 0} \left(\int_0^{\omega - \delta} \frac{1}{s^2 - \omega^2} ds + \int_{\omega + \delta}^\infty \frac{1}{s^2 - \omega^2} ds \right)$$

$$= \lim_{\delta \to 0} \left(\frac{1}{2\omega} \ln \left| \frac{s - \omega}{s + \omega} \right| \right) \Big|_0^{\omega - \delta} + \lim_{\delta \to 0} \left(\frac{1}{2\omega} \ln \left| \frac{s - \omega}{s + \omega} \right| \right) \Big|_{\omega + \delta}^\infty = 0 \tag{9}$$

Equation (9) means that adding a constant, like $\ln R(\omega)$, to the numerator in the integral equation (7) does not change the integration result, because

$$p\int_0^\infty \frac{\ln R(\omega)}{s^2 - \omega^2} ds = 0 \tag{10}$$

Therefore, the integral equation (7) can be written in the following form

$$\theta(\omega) = -\frac{\omega}{\pi} p \int_0^\infty \frac{\ln R(s) - \ln R(\omega)}{s^2 - \omega^2} ds \tag{11}$$

To calculate the integral equation (11), two problems need to be solved, one is the integral equation (11) calculation needs reflection spectrum $R(\omega)$ at $\omega \in [0,\infty]$, theoretically. But obviously, the range of reflection spectrum measured by a spectrometer is usually only near the visible band, cannot cover the entire wavelength range. In this paper, the wavelength range of the experimental data is $200nm \leq \lambda \leq 900nm$, the corresponding frequency range is

$2.0944 \times 10^{14} \ rad/s \le \omega \le 9.4248 \times 10^{14} \ rad/s$. Reflection spectrum values outside the range

can only be extrapolated by some extrapolation particular methods on the basis of the optical properties of the BAM material. In the short wavelength region, the reflectance spectrum can be extrapolated by exponential decay method. In the long wavelength region, the reflection spectrum does not change with frequency, so the spectrum can be extrapolated by constant method.